IEEE Access
Multidisciplinary | Rapid Review | Open Access Journal

Received October 27, 2018, accepted November 10, 2018, date of publication November 14, 2018,
date of current version December 18, 2018.

Digital Object Identifier 10.1109/ACCESS.2018.2881290

Bi-Level Programming Model for Dynamic Reversible Lane Assignment

TING LU[1], ZHONGZHEN YANG[1], DONGFANG MA[2], AND SHENG JIN[3]
[1]Faculty of Maritime and Transportation, Ningbo University, Ningbo 315211, China
[2]Institute of Marine Sensing and Networking, Zhejiang University, Zhoushan 316021, China
[3]College of Civil Engineering and Architecture, Zhejiang University, Hangzhou 310058, China

Corresponding author: Zhongzhen Yang (yangzhongzhen@nbu.edu.cn)

This work was supported in part by the Zhejiang Provincial Natural Science Foundation of China under Grant LQ18F030004, in part by the National Natural Science Foundation of China under Grant 71431001, and in part by Ningbo University through the K. C. Wong Magna Fund.

ABSTRACT To improve the space utilization and traffic capacity of a signalized junction, this paper proposes a dynamic reversible lane assignment method for approaches of signalized junctions that consider the game equilibrium between road users and traffic controllers. To theoretically analyze the behaviors of the players involved in the leader-follower strategic game, a bi-level programming model is established. To minimize the total queue length of approaches at signalized junctions, the upper model dynamically optimizes the reversible lane assignments and can be solved with the enumeration method or the Monte Carlo algorithm. The lower model outputs the traffic assignment at road sections using a Logit-based stochastic user equilibrium model that is solved by the method of successive averages. The general impedance of road section in lower model consists of the road travel time cost and the intra-time cost at the signalized junction connected with current road section. In addition, the interaction between the two levels is simulated in an iterative optimization procedure. Finally, this paper uses two numerical experiments to validate the proposed approach.

INDEX TERMS Bi-level programming, queue length, reversible lane, stochastic user equilibrium, traffic engineering.

I. INTRODUCTION

The junctions of a road network are important nodes. The spatial and temporal optimization of junctions is thus critical for guaranteeing smooth and safe urban traffic flow. Setting reversible lanes can significantly improve the space usage of a junction. Based on the periodicity and real-time attributes of traffic flow, the driving direction(s) at junction lane(s) can be reversed dynamically using traffic engineering and computer controlling actions, which allows for more reasonably and effective road space use. As a result, traffic flows through a junction can be adjusted and the junction capacity can be improved [1]. Under the reversible lane mechanism, the desired driving directions at junctions' approaches or channelized sections can be reversed with the change of traffic flows into and out of the junction. Therefore, the dynamic assignment of reversible approach lanes can make full use of road space and alleviate the conflict between periodically changeable heavy traffic and fixed approach lane assignment of a junction. Implementing dynamic assignment of reversible approach lanes can release the road capacity of an urban traffic network and reduce traffic congestion.

The dynamic reversible lane assignment technique is applicable to various classified roads. Without any large changes to road structure, controlling facility or traffic infrastructure, dynamic reversible lanes can greatly improve road capacity [2]–[4]. Effectiveness, feasibility and safety issues of implementing lane reversal have been discussed in, for example, Hemphill and Surti [5], Waleczek *et al.* [6]. Reversible lanes have been widely used in many scenarios with unbalanced bi-directional traffic including tidal rush hour traffic flow [7], [8], emergency rescue [9]–[12], and temporary road maintenance [13]–[16]. The reversible strategy becomes more widely accepted mainly for the emergency evacuation.

The reversibility strategy is a traffic management method, which essentially accommodates the unbalanced traffic flows between two driving directions on a congested roadway section during daily peak periods. Researchers provided many controlling method and strategies of the reversible

lanes. Tuydes and Ziliaskopoulos [17], [18] formulated the system-optimal dynamic traffic assignment (SODTA)-based capacity reversibility problem as a linear program, which propagates traffic based on the cell transmission model (CTM) to better represent vehicle-level movements, to capture spatiotemporal changes in disaster conditions, and to enable optimal capacity reversibility calculation. The deficiencies of lane-based capacity-reversibility models are on the cost of the street divisions and the risk in assigning contradicting flows on the same highway. Karoonsoontawong and Lin*et al.* [8] proposed a time-varying lane-based capacity reversibility (TVLCR) model based on the user-optimal dynamic traffic assignment (UODTA) for peak-period traffic management on a daily basis. The model embedded the cell transmission model (CTM) that can capture traffic realisms such as shockwaves and spillovers. Xie and Turnquist [19], [20] established and solved a model for the evacuation network optimization problem by integrating lane reversal and crossing point elimination strategies. Xie et al. assume drivers do not receive instructions from the roadway manager and behave in a user-optimal manner, and also assume static reversibility, and developed a Lagrangian relaxation-based Tabu search. Kalafatas and Peeta [16] proposed an optimal lane reversal model constrained by a limited set of crossing elimination designs, in which the crossing elimination setting at each intersection is treated as selection of turning movements from a pre-specified allowable set. Xu *et al.* [21] proposed a hybrid dynamic lane operation that can automatically adjust the direction of tide lanes and reversible lanes based on road structure, traffic controlling facilities and predominant driving direction changes. Zhang and Gao [22] built a discrete bi-level programming model to adjust the lane assignment of road sections where traffic flows in each direction are disequilibrium. Sheu and Ritchie [23] analyzed the potential of applying lane reversal techniques to alleviate temporary congestion caused by traffic incidents and formulated a discrete-time nonlinear stochastic model with estimation of lane-changing fractions for real-time incident management. Zhao *et al.* [24] presented an innovative design and operational model for signalized diamond interchanges by dynamically reversing certain lanes in the internal link on a regular basis with the deployment of overhead reversible lane control signs. Krause *et al.* [25] studied the advantages of using dynamic reversible lanes for left-turn movements at the signalized diamond interchange of freeway-to-arterial connections. Asia and Ratroutb [26] proposed a quick method of finding the optimum lane group for 3-lane and 4-lane approaches at junctions where each approach in turn is given its green light using the percentage of turning movements. It was achieved by developing massive hypothetical data sets of turning volumes (more than 600,000 data sets) for the typical intersection. Wong and Wong [27] developed a binary-mix-integer linear optimization model to integrate the design of lane markings and signal timing settings for isolated junctions. They considered two objectives: capacity maximization and cycle length minimization. Using several numerical examples, they concluded that their optimization method enhanced the junction operation by increasing the reserve capacity up to 48%.

However, in the above studies and practices, the number and driving direction of reversible lanes are fixed, which can neither maximize the effect of reversible lanes nor make the best use of road space resource. Although constant changes of canalization direction have a negative effect on driving, dynamic reversible lane assignment has become more realizable with the development of driver assistance systems and automatic drive technology [28]–[30]. Furthermore, dynamic reversible lane assignment is meaningful for public transit, car ride sharing and automated vehicles. Based on the behaviors of traffic supply and demand over road networks and the traffic equilibrium theory, this paper proposes a method of dynamic reversible lane assignment that is formulated using a bi-level programming model that involves Stochastic User Equilibrium (SUE) [31], [32]. The bi-level programming optimization has increasingly appeared in the transportation field [33]–[37]. In this paper, the upper model of the bi-level programming minimizes the total queue length at junctions' approaches to find the optimal assignment of reversible lanes, while the lower model is a traffic assignment model based on stochastic user equilibrium and is solved by the successive averages algorithm. This paper uses two numerical studies for model validation.

II. DYNAMIC REVERSIBLE LANE ASSIGNMENT MODEL

In proposed the bi-level model, the upper model is built for optimizing reversible lane assignment by computing and comparing the total queue length at junctions' approaches. The lower model is the traffic assignment model based on stochastic user equilibrium, which assigns travel routes and outputs traffic flows on the road sections. The model assumptions are as follows:

(1) All drivers are able to obtain lane reversal information in advance and driving behaviors are free from the effect of canalization changes.

(2) OD demands are known in the study area.

A. UPPER MODEL

$$minZ_u\left(q_a^i, k_a^i\right) = \sum_{a\in A\cap N^a\in I}\sum_{i\in M_a} H_a^i \tag{1}$$

Here, Z_u is the average queue length at junctions' approaches, H_a^i is the average queue length (measured by vehicle count) of direction i at approach a, q_a^i is the flow rate (vehicles/hour) of direction i at approach a, k_a^i is the lane counts of direction i at approach a, A is the set of approaches in the road networks, n_a is the lane count of approach a, N^a is the downstream node of road section a, I is the set of signalized junctions in the road network, and M_a is the set of flow directions at approach a.

Researchers have proposed many of approaches to calculate queue length, such as Miller, Akcelik, SYNCHRO 3, SIGNAL 94, and TRANSYT [38]. Here, the classical Akcelik

model is employed to compute the queue length at a junction's approaches [39] as follows:

$$H_a^i = \begin{cases} q_a^i r_a^i + \dfrac{exp\left[-1.33\sqrt{s_a^i g_a^i}\left(1-\chi_a^i\right)/\chi_a^i\right]}{2\left(1-\chi_a^i\right)}, & 0 \le \chi_a^i < 1 \\ s_a^i \lambda_a^i r_a^i + 0.5 s_a^i \lambda_a^i T\left(\chi_a^i - 1\right), & \chi_a^i \ge 1 \end{cases} \tag{2}$$

s.t.

$$r_a^i + g_a^i = C^a, \quad \forall a \in A,\ N^a \in I,\ i \in M_a \tag{3}$$

$$\lambda_a^i = \frac{g_a^i}{C^a}, \quad \forall a \in A,\ N^a \in I,\ i \in M_a \tag{4}$$

$$s_a^i = s k_a^i, \quad \forall a \in A,\ N^a \in I,\ i \in M_a \tag{5}$$

$$\chi_a^i = \frac{q_a^i}{s_a^i \lambda_a^i}, \quad \forall a \in A,\ N^a \in I,\ i \in M_a \tag{6}$$

$$1 \le k_a^i \le n_a \cap k_a^i \in N, \quad \forall a \in A,\ N^a \in I,\ i \in M_a \tag{7}$$

$$\sum_{i \in M_a} k_a^i = n_a, \quad \forall a \in A,\ N^a \in I \cup 0.5 \tag{8}$$

$$q_a^i \ge 0, \quad \forall a \in A,\ N^a \in I,\ i \in M_a \tag{9}$$

$$\chi_a^i \ge 0, \quad \forall a \in A,\ N^a \in I,\ i \in M_a \tag{10}$$

Equation (8) is the constraint that guarantees each directional traffic flow has independent right-of-way. r_a^i is the red time (hours) of direction i at approach a, s_a^i is the saturate flow rate (vehicles/hour), which is equal to the product of single-lane saturate flow rate (s) and the lane count of direction i at approach a (k_a^i), g_a^i is the effective green time (hours) of direction i at approach a, C^a is the cycle time (hours) of the signalized junction at approach a, χ_a^i is the saturation of direction i at approach a, λ_a^i is the green split of direction i at approach a, and T is the study time span (hours).

B. LOWER MODEL

The lower model is a Logit-based Stochastic User Equilibrium model for traffic assignment, which is formulated as follows:

$$min\ Z_L(f) = \sum_{a \in A} \int_0^{q_a} \left[t_a(x) + d_a(x)\right] dx + \frac{1}{\theta} \sum_{w \in W} \sum_{r \in R_W} f_r^w \ln f_r^w \tag{11}$$

$$\text{s.t.} \sum_{r \in R_w} f_r^w = e_w, \quad \forall w \in W \tag{12}$$

$$f_r^w \ge 0, \quad \forall r \in R_w,\ w \in W \tag{13}$$

$$\sum_{w \in W} \sum_{r \in R_w} f_r^w d_{a,r}^w = q_a, \quad \forall a \in A \tag{14}$$

Here, $Z_L(f)$ is the objective function, θ denotes traveler perception degree of impedance, which is inversely proportional to perception error, f_r^w is the traffic flow along Route r between OD pair w, and e_w is the traffic demand of OD pair w.

A road network can be presented by a weighted directed graph G(N, A, I) in which N is the node set, A is the road section set and I is the signalized junction set. The impedance function consists of a deterministic term and the stochastic error, which is shown in (15) and (16). The stochastic error term follows the Gumble distribution.

$$c_r^w(f) = \sum_a c_a(q_a) \delta_{a,r}^w + \xi_r^w \tag{15}$$

$$c_a(q_a) = t_a(q_a) + d_a(q_a) \tag{16}$$

Here, c_r^w is the general travelling impedance on Route r between OD pair w, and $\delta_{a,r}^w$ is a 0-1 parameter of Route r between OD pair w, where road section a on Route r is 1 and otherwise $\delta_{a,r}^w$ is 0. ξ_r^w is the stochastic error, $c_a(q_a)$ is the general impedance of road section a, and $t_a(q_a)$ is the traveling time cost on road section a, which can be calculated with the BPR functions as follow [40]:

$$t_a(q_a) = t_{0a}\left[1 + \alpha\left(\frac{q_a}{Q_a}\right)^\beta\right] \tag{17}$$

Here, t_{0a} is the free flow time on road section a, q_a is the traffic flow (vehicles/hour) on road section a, Q_a is the traffic capacity (vehicles/hour) of road section a, and α, β are constant parameters (usually $\alpha = 0.15$, $\beta = 4$).

In (16), $d_a(q_a)$ is the intra-time cost at the signalized junction connected with road section a, and $d_a(q_a)$ can be computed by the Webster delay model as follows [41], [42]:

$$d_a(q_a) = \sum_{i \in M_a} d_a^i q_a^i / q_a \tag{18}$$

$$d_a^i = \begin{cases} \dfrac{C^a\left(1-\lambda_a^i\right)^2}{2\left(1-\lambda_a^i \chi_a^i\right)} + \dfrac{\left(\chi_a^i\right)^2}{2q_a^i\left(1-\chi_a^i\right)} - 0.65\left[\dfrac{C^a}{\left(q_a^i\right)^2}\right]^{\frac{1}{3}} \\ \left(\chi_a^i\right)^{2+5\lambda_a^i}, 0 \le \chi_a^i < 1 \cap N^a \in I \\ \dfrac{R_a^i}{2} + \dfrac{T\left(\chi_a^i - 1\right)}{2}, \chi_a^i > 1 \cap N^a \in I \\ 0, N^a \notin I \end{cases} \tag{19}$$

Here, I is the junction set, N^a is the downstream node of road section a, and d_a^i is the average time cost (hours/vehicle) of direction i at road section a. If the downstream node of a is signalized junction, the first two equations in (19) are used to compute d_a^i; otherwise, $d_a^i = 0$ (the last equation in (19)). q_a^i is the flow rate (vehicles/hour) of direction i at road section a, λ_a^i is the green split of direction i at road section a, χ_a^i is the saturation of direction i at road section a, C^a is the cycle time (hours) of the signalized junction connected with road section a, and M_a is the direction set of road section a.

Applying the Lagrange relaxation to the lower model, the Lagrange function can be obtained as follows:

$$L = Z_L + \sum_{w \in W} \mu_w \left(e_w - \sum_{r \in R_w} f_r^w\right) - \sum_{w \in W} \sum_{r \in R_w} v_r^w f_r^w \tag{20}$$

Here, μ_w and v_r^w are Lagrange multipliers corresponding to the constraints. According to the Kuhn-Tucher conditions, the extreme point of the Lagrange function (20) satisfies the following conditions:

$$\frac{\partial L}{\partial f_r^w} = 0, \quad \frac{\partial L}{\partial \mu_w} = 0, \quad \frac{\partial L}{\partial v_r^w} = 0 \tag{21}$$

which can be transformed to:

$$\frac{\partial L}{\partial f_r^w} = c_r^w + \frac{1}{\theta}\ln f_r^w - \mu_r^w = 0 \tag{22}$$

So the flow on Route r between OD w can be determined as:

$$f_r^w = exp\left[-\theta\left(c_r^w - \mu_r^w\right)\right] \tag{23}$$

Substituting (23) into constraint (12), the equilibrium flow on Route r between OD w can be finally obtained as follows:

$$f_r^{w*} = e_w \frac{exp\left(-\theta c_r^w\right)}{\sum\limits_{j\in R_w} exp\left(-\theta c_j^w\right)}, \quad \forall r \in R_w,\ w \in W \tag{24}$$

Equation (24) also proves that traveler route choice behavior follows the Logit model.

III. SOLUTION ALGORITHMS FOR BI-LEVEL PROGRAMMING MODEL

A. ALGORITHM DESIGN

To solve the bi-level programming model, this paper uses an iteration algorithm which is described as follows [43]:

Step 1 (Initialization): Set the iteration counts $n = 1$. Set $d_a\left(q_a\right)^{(1)} = 0$ (ignoring the intra-time cost in junctions). Solve the lower model and obtain route flow $f_r^{w(1)}$ and road section flow $q_a^{(1)}$.

Step 2 (Solve the Upper Model): Substitute the route flow $f_r^{w(n)}$ and road section flow $q_a^{(n)}$ into the upper model to compute the flows of each direction at approaches of signalized junctions and find the optimal reversible lane assignment in iteration n. Compute the intra-junction time cost $d_a\left(q_a\right)^{(n)}$.

Step 3 (Solve the Lower Model): Set $n = n + 1$. Substitute $d_a\left(q_a\right)^{(n-1)}$ (the intra-junction time cost in iteration $n-1$) into the impedance function to solve the lower model and obtain the route flow $f_r^{w(n)}$ and road section flow $q_a^{(n)}$ in iteration n.

Step 4 (Stop Iteration): If the change rate of the objective function value of 2 successive iterations is less than the preset convergence precision, then the iteration procedure will be stopped and the optimal reversible lane assignment will be output; otherwise, go to step 2.

B. UPPER MODEL SOLUTION ALGORITHM

The upper model uses multi-variable nonlinear programming which can be solved with the enumeration method when the road network is small. When the road network is large and the number of variables is high, the problem can be solved with the Monte Carlo algorithm as follows:

Step 1: Set iteration $j = 1$. Set maximum iteration $j_{\max}$. Randomly generate m feasible solutions $k_a^{i(j)}$ and compute the corresponding objective function values.

Step 2: Find the optimal feasible solution by sorting m objective function values in descending order. Set this best objective function value as $Z_u^{(j)}$.

Step 3: According to the probability distribution of the first n feasible solutions in descending order, generate $m-n$ feasible solutions $k_a^{i(j+1)}$. The new feasible solution set is composed of $m-n$ feasible solutions $k_a^{i(j+1)}$ and the n feasible solutions $k_a^{i(j)}$.

Step 4: Find the best objective function value $Z_u^{(j+1)}$ from the new feasible solution. If the objective function value difference between 2 iterations is less than the convergence precision ε, *i.e.*, $Z_u^{(j+1)} - Z_u^{(j)} < \varepsilon$, then the iteration procedure will be stopped; otherwise, set $j = j + 1$ and check whether the iteration count reaches $j_{\max}$. If $j < j_{\max}$, go to Step 3; otherwise, the iteration procedure will be stopped.

C. LOWER MODEL SOLUTION ALGORITHM

The lower model is solved by the Method of Successive Averages (MSA) based on road section flow. The MSA procedure starts with a preset iteration step sequence $\{\kappa_n\}$ where the iteration count $n = 1, 2, \ldots$. To guarantee the convergence of MSA, the iteration step sequence must follow the condition $\sum\limits_{n=1}^{\infty}\kappa_n = \infty$, $\sum\limits_{n=1}^{\infty}(\kappa_n)^2 < \infty$, and the solution search direction is descent. Sheffi proved that the descent expectation direction is adequate for guaranteeing the convergence of MSA even though the search direction is stochastic in each iteration [33], [44]. If the iteration step sequence $\kappa_n = \left\{\frac{1}{n}\right\}$, MSA procedure is described as follows:

Step 1(Initialization): Set the iteration count $n = 1$. Initialize $t_a^{(1)}$. Randomly load route flows onto the road network and obtain the initial road section flow $q_a^{(1)}$.

Step 2 (Update Road Section Impedance): Set iteration count $n = n + 1$. According to road section flow $q_a^{(n)}$, update impedance $c_a^{(n)} = c_a\left(q_a^{(n)}\right)$.

Step 3(Determine Search Direction): According to impedance $c_a^{(n)}$ and (24) , assign OD demands to routes and obtain the additional road section flow $\overline{q_a^{(n)}}$. Set the search direction as the direction of $\overline{q_a^{(n)}} - q_a^{(n)}$.

Step 4(Update Road Section Flow): The new road section flow $q_a^{(n+1)} = q_a^{(n)} + \left(\overline{q_a^{(n)}} - q_a^{(n)}\right)/n$.

Step 5(Stop the Iteration): If the change rate of road section flows between 2 iterations is less than the convergence precision, *i.e.* $\sqrt{\sum\limits_{a\in A}\left(q_a^{(n)} - q_a^{(n-1)}\right)^2} / \sum\limits_{a\in A} q_a^{(n-1)} \le \varepsilon$, then the iteration procedure will be stopped and the traffic flow assignment will be output; otherwise, go to Step 3.

IV. NUMERICAL EXPERIMENTS

A. NUMERICAL EXPERIMENT 1

The road network 1 in the first experiment is presented as Fig. 1. The impedance function on each road section is tagged in the figure. Road section AB, AC, BD, and CD are all 1-direction 3-lane roads, and road section BC, CB are bi-directional, 6-lane roads. The saturate flow rate of a lane is 1700 vehicles/hour. There is only 1 OD pair OD_{AD} in this experiment. The demand of OD_{AD} is 1000. There are 4 Routes from origin A to destination D, i.e., ABD (Route 1), ACD (Route 2), ABCD (Route 3) and ACBD (Route 4).

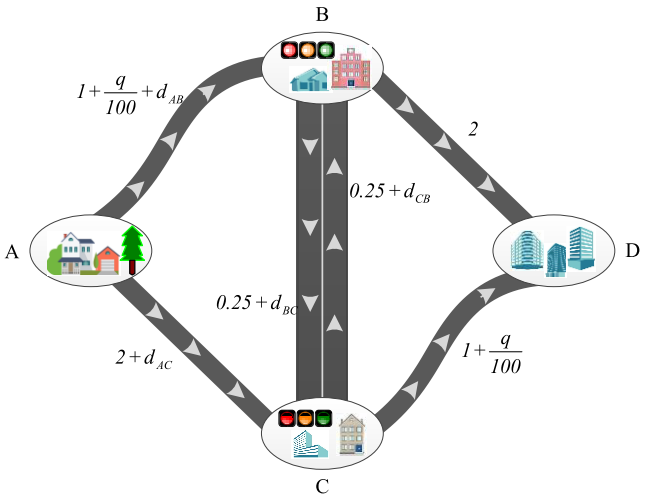

FIGURE 1. Road network of experiment 1.

TABLE 1. Signal timing plans of Junctions B and C.

Junction	Phase 1	Phase 2	Cycle Time (s)	Green Time (s)		Green Split	
				g_1	g_2	λ_1	λ_2
B			70	40	20	0.57	0.29
C			60	30	20	0.5	0.33

Nodes B and C are signalized junctions, which have two phases. The phases, phase sequence and signal timing plans for which are presented in Table 1. g_1 and g_2 denote the green time of phase 1 and phase 2. λ_1 and λ_2 denote the green split of phase 1 and phase 2.

In the lower model, θ is traveler perception to road impedance; the smaller the variance of traveler perception, the larger the θ value and the faster the convergence of the algorithm. And conversely, the larger the variance of traveler perception, the smaller the θ value. Here, it is assumed that the travelers are well aware of the impedance and the variance of the perception is small. Thus, in this experiment, θ is set as 10. After 3 iterations, the algorithm is converged. The low traffic demand in this experiment is another reason for fast convergence. The output results of each iteration, including the route flows, the number of lanes at approaches of junctions B and C, the average network impedances are listed in Table 2.

As θ varies, iteration count, route flow and average impedance vary, as shown in Table 3. As θ increases, the algorithm converges faster and the average impedance (represented as Avg. Imp.) decreases. When $\theta \geq 0.5$, the average impedance stabilizes. When $\theta \geq 0.8$, the flows of Route ABCD and ACBD remain 0, and the OD demand is always assigned to Routes ABD and ACD.

TABLE 2. Outputs of each calculation iteration.

Outputs		Iteration		
		1	2	3
Route Flow (vehicles)	f_1	141.4	663.34	495.32
	f_2	141.4	336.66	504.68
	f_3	0.18	0	0
	f_4	717.02	0	0
Number of Lane	AB Straight	2	2	2
	AB Right	1	1	1
	CB Right	3	3	3
	AC Straight	1	2	2
	AC Left	2	1	1
	BC Left	3	3	3
Average Impedances(s)		29	17.01	16.52

TABLE 3. Route flow, iteration count and average impedance for several values of θ.

θ	Iteration	f_1	f_2	f_3	f_4	Ave. Imp. (s)
0.1	5	436.10	397.77	74.82	91.32	18.68
0.2	5	508.50	450.88	15.84	24.78	16.96
0.3	5	529.05	461.94	2.98	6.04	16.59
0.4	5	534.71	463.32	0.54	1.42	16.52
0.5	4	540.41	459.17	0.10	0.32	16.50
0.6	4	543.20	456.70	0.02	0.07	16.50
0.7	3	526.26	473.72	0.00	0.02	16.50
0.8	3	525.54	474.45	0.00	0.00	16.50
0.9	3	524.78	475.22	0.00	0.00	16.50
1	3	524.38	475.62	0.00	0.00	16.50
3	3	516.88	483.12	0.00	0.00	16.50
5	3	507.67	492.33	0.00	0.00	16.51
7	3	503.78	496.22	0.00	0.00	16.51
10	3	504.68	495.32	0.00	0.00	16.52

Fig. 2 displays the relationships of θ, the converged route flow the average impedance (Avg. Imp.). For a fixed road capacity, the OD demand e_w can indicate the congestion level of the road network. The larger e_w, the more serious the congestion. When the demand is low, the change of impedance expectations between 2 successive iterations and the traffic assignment results hardly change, and thus the algorithm converges faster; the inverse case, i.e., with high traffic demand and slow convergence, is also true. In this experiment, the OD demand is not high and the algorithm converges quickly.

To assess the benefits of several scenarios based on travel demand information, we use the formulation proposed by Chen and Kempe [45]. Although a driver experiences and considers only his/her own travel time, the cost of the entire

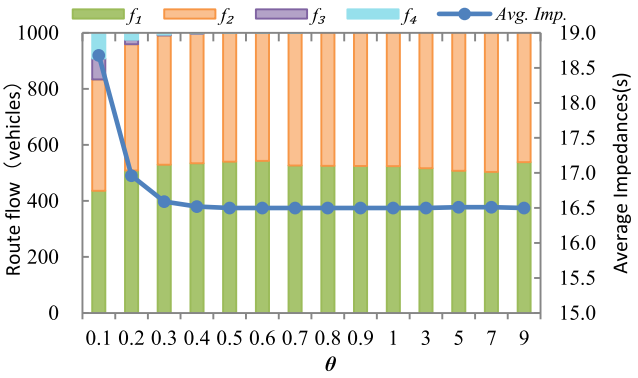

FIGURE 2. Relationships among θ, converged route flow and average impedance.

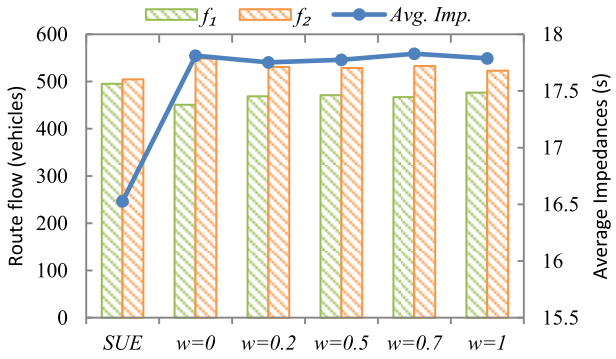

FIGURE 3. Route flow and average impedance.

system also includes the marginal cost of the driver imposes on all other drivers on the road segments he/she takes. The cost function of a driver is a linear combination of the cost he/she will incur and the total marginal cost his/her choice imposes on everyone else, i.e.

$$\begin{aligned} & c_a^w(q_a) \\ &= (1-w)\left[t_a(q_a)+d_a(q_a)\right] + w\frac{\partial\left[q_a t_a(q_a)+q_a d_a(q_a)\right]}{\partial q_a} \\ &= \left[t_a(q_a)+d_a(q_a)\right] + wq_a\frac{\partial\left[t_a(q_a)+d_a(q_a)\right]}{\partial q_a} \end{aligned} \tag{25}$$

Here, $w \in [0, 1]$ defines the weight of social good, which ranges between 0 and 1. $w = 0$ indicates a driver considers only the cost of his/her route and potentially moves the system away from optimality. The set of flows that occur when every driver minimizes their own travel time is referred to as the user equilibrium flows. Theoretically, in the resulting system state, no driver can benefit from deviating from their route. This idea, essentially describing a Nash equilibrium in roads, is captured in Wardrop's principles in transportation [46], [47]. $w = 1$ indicates the driver chooses routes with respect to marginal costs, thus moving the system closer to the system optimum. The resulting convex programming for the socially aware routing problem is as follows:

$$min \sum_{a \in A} \int_0^{q_a} c_a^w(x) \cdot x dx \tag{26}$$

TABLE 4. Road section specifications.

Road	O	D	Lane Num.	Free Flow Time (s)	Len.	Road	O	D	Lane Num.	Free Flow Time (s)	Len.
1	1	2	3	21.6	360	26	13	14	1	13.8	230
2	1	8	3	12.0	200	27	13	20	1	12.6	210
3	2	1	3	21.6	360	28	14	16	1	6.0	100
4	2	3	3	6.0	100	29	15	13	1	6.0	100
5	2	9	1	12.0	200	30	15	16	1	13.8	230
6	3	2	3	6.0	100	31	16	7	1	6.0	100
7	3	4	3	4.2	70	32	17	8	3	14.4	240
8	4	3	3	4.2	70	33	18	17	1	19.8	330
9	4	5	3	6.6	110	34	18	22	3	13.2	220
10	4	11	1	12.0	200	35	19	12	1	13.2	220
11	5	4	3	6.6	110	36	19	18	1	18.0	300
12	5	6	3	12.6	210	37	20	19	1	12.0	200
13	6	5	3	12.6	210	38	20	24	1	9.0	150
14	6	7	3	13.8	230	39	21	14	1	12.0	200
15	6	15	3	6.0	100	40	21	20	1	13.8	230
16	7	6	3	13.8	230	41	22	18	3	13.2	220
17	8	1	3	12.0	200	42	22	23	3	18.0	300
18	8	9	1	19.8	330	43	23	19	3	12.0	200
19	8	17	3	14.4	240	44	23	22	3	18.0	300
20	9	10	1	6.6	110	45	23	24	3	12.0	200
21	9	18	3	13.8	230	46	24	20	3	9.0	150
22	10	3	1	12.0	200	47	24	23	3	12.0	200
23	10	11	1	3.6	60	48	24	25	3	14.4	240
24	12	5	1	12.0	200	49	25	21	3	6.0	100
25	12	13	1	12.6	210	50	25	24	3	14.4	240

Note: Lane Num. denotes the number of lane, and Len. denotes the length of road section.

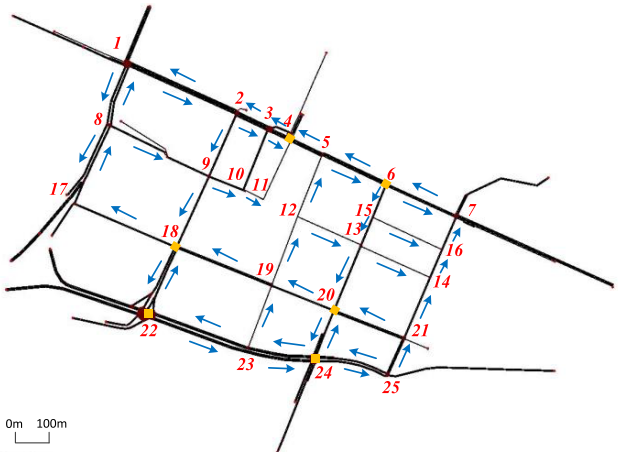

FIGURE 4. Road network of experiment 2.

In the above experiment, the optimized lane assignment schemes do not change with different traffic assignment models. Therefore, the optimized result is independent of the traveler route choice behavior described in the lower model. Travelers always prefer Route ABD and ACD while Route ABCD and ACBD are not chose. The equilibrium flow and average network impedance of Route ABD and ACD with

TABLE 5. Routes between OD(1, 25) and OD(25,1).

OD	Route ID	Nodes on the route
(1, 25)	1	1-2-3-4-5-6-15-13-20-24-25
	2	1-2-9-18-22-23-24-25
	3	1-2-9-18-22-23-19-12-13-20-24-25
	4	1-8-9-10-3-4-5-6-15-13-20-24-25
	5	1-8-9-18-22-23-24-25
	6	1-8-9-18-22-23-19-12-13-20-24-25
(25, 1)	1	25-24-23-22-18-17-8-1
	2	25-24-23-22-18-17-8-9-10-3-2-1
	3	25-24-23-19-12-5-4-3-2-1
	4	25-24-23-19-18-17-8-1
	5	25-24-20-19-12-5-4-3-2-1
	6	25-24-20-19-18-17-8-1
	7	25-21-14-16-7-6-5-4-3-2-1
	8	25-21-20-19-18-17-8-1
	9	25-21-20-19-12-5-4-3-2-1

different traffic assignment models are displayed in Fig. 3. From Fig.3 it can be observed that the flow on Route ABD and ACD are not very different. The difference between the two route flows calculated with SUE model is the smallest among all traffic assignment models, and the average impedance per vehicle is also the smallest (16.52 s). The average impedance computed by the User Equilibrium model ($w = 0$) is 17.81 s, and that computed by the System Optimization model ($w = 1$) is 17.79 s. Therefore, according to the traffic assignment and the reversible lane scheme optimized by the proposed model, the average impedance per vehicle can be reduced by approximately 1.3 s (7.8%) compared to other models.

B. NUMERICAL EXPERIMENT 2

The road network used for experiment 2 is presented in Fig. 4. There are 25 nodes including 6 signalized junctions which are Nodes 4, 6, 18, 20, 22 and 24. There are 50 road sections. All bi-directional road sections are 6-lane roads and all one-directional road sections are single-lane roads. The specifications of the road sections are listed in Table 4.

There are 2 pairs of OD demands: OD(1,25) and OD(25,1). There are 6 routes from origin node 1 to destination node 25 and 9 reverse routes. Table 5 lists the alternative routes between the two ODs.

The junction 4 and 6 has two phases, junction 18 and 20 has three phases, and junction 22 and 24 has four phases. Table 6 shows the phase sequences and signal timing plans of the six signalized junctions.

The output optimal lane assignment by the proposed model is listed in Table 7. The lane assignment is related to the traveler impedance perception (θ), because the travel impedance perception is strongly related to the route flow assignment, which determines the traffic flow at junction approaches.

The equilibrium flows on each route between the two OD pairs are displayed in Fig. 5. The traffic demand of OD(1,25)

TABLE 6. Parameters of the 6 signalized junctions in experiment 2.

Jun.	Phase 1	Phase 2	Phase 3	Phase 4	Cycle Time (s)	Green Time (s)			
						g_1	g_2	g_3	g_4
4			-	-	70	30	30	-	-
6			-	-	60	20	30	-	-
18, 20				-	85	30	20	20	-
22, 24					90	20	15	20	15

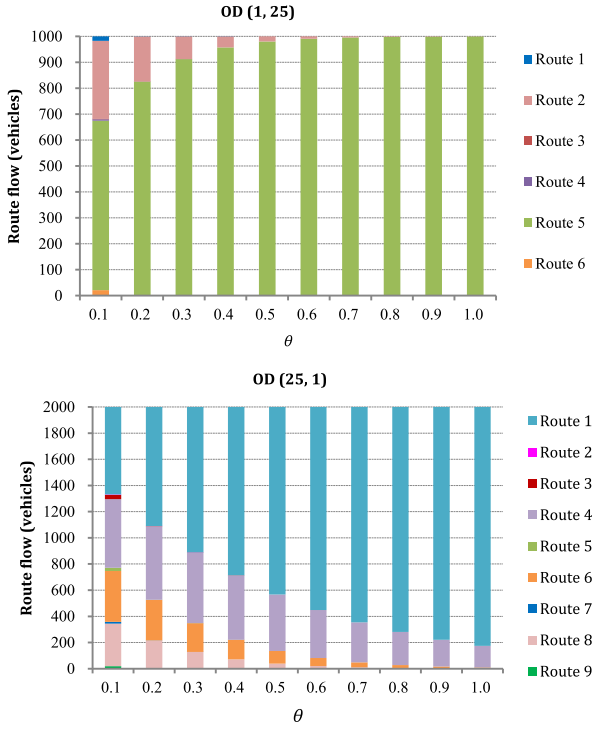

FIGURE 5. Flows on the routes between the 2 ODs.

is mainly assigned to Route 2 and Route 5. When $\theta \geq 0.6$, almost every traveler chooses Route 5. The traffic demand of OD(25,1) is mainly assigned to Routes 1, 4, 6 and 8. With θ increasing, the flow on Route 1 increases but those on other routes decrease. When $\theta = 1.0$, all travelers choose Route 1 or Route 4.

The flow distribution is shown as Fig. 6 for θ values of 0.2 and 1.0, where the solid lines denote flows on the routes between OD(1,25), while the dotted lines depict flows on the routes between OD(25,1). Moreover, the thicker line, the more flows on the route. It can be observed in Fig. 6 that few travelers choose one-way road sections.

TABLE 7. Optimal lane assignment.

Jun.	Dir.	θ									
		0.1	0.2	0.3	0.4	0.5	0.6	0.7	0.8	0.9	1
4	EB-L	0.5	1	1	1	0.5	1	1	1.5	2	1
	EB-S	0.5	1.5	0.5	1.5	0.5	1	1	0.5	0.5	1.5
	EB-R	2	0.5	1.5	0.5	2	1	1	1	0.5	0.5
	WB-L	0.5	1	1	1.5	0.5	1	0.5	0.5	2	0.5
	WB-S	2	1	0.5	1	0.5	1	2	2	0.5	1.5
	WB-R	1	1	1.5	0.5	2	1	1	1	0.5	1
6	EB-S	2	0.5	2	1.5	1.5	2	2.5	2.5	2.5	2.5
	EB-R	1	2.5	1	1.5	1.5	1	0.5	0.5	0.5	0.5
	WB-L	2	1	2	1	1.5	2	0.5	1	1	0.5
	WB-S	1	2	1	2	1.5	1	2.5	2	2	2.5
18	NB-L	3	3	3	3	3	3	3	3	3	3
	WB-L	0.5	0.5	0.5	0.5	0.5	0.5	0.5	0.5	0.5	0.5
	WB-S	0.5	0.5	0.5	0.5	0.5	0.5	0.5	0.5	0.5	0.5
	SB-S	0.5	0.5	0.5	0.5	0.5	0.5	0.5	0.5	0.5	0.5
	SB-R	0.5	0.5	0.5	0.5	0.5	0.5	0.5	0.5	0.5	0.5
20	NB-L	3	3	3	3	3	3	3	3	3	3
	WB-L	0.5	0.5	0.5	0.5	0.5	0.5	0.5	0.5	0.5	0.5
	WB-S	0.5	0.5	0.5	0.5	0.5	0.5	0.5	0.5	0.5	0.5
	SB-S	0.5	0.5	0.5	0.5	0.5	0.5	0.5	0.5	0.5	0.5
	SB-R	0.5	0.5	0.5	0.5	0.5	0.5	0.5	0.5	0.5	0.5
22	WB-L	0.5	0.5	0.5	0.5	0.5	0.5	0.5	0.5	0.5	0.5
	WB-S	0.5	0.5	0.5	0.5	0.5	0.5	0.5	0.5	0.5	0.5
	WB-R	2	2	2	2	2	2	2	2	2	2
	SB-L	2	1.5	2	2	2	2	2	2	2	2
	SB-S	0.5	1	0.5	0.5	0.5	0.5	0.5	0.5	0.5	0.5
	SB-R	0.5	0.5	0.5	0.5	0.5	0.5	0.5	0.5	0.5	0.5
24	EB-L	0.5	0.5	0.5	0.5	0.5	0.5	0.5	0.5	0.5	0.5
	EB-S	2	2	2	2	2	1.5	2	1.5	2	2
	EB-R	1	1	1	1	1	1	1	1	1	1
	WB-L	0.5	0.5	0.5	0.5	0.5	0.5	0.5	0.5	0.5	0.5
	WB-S	2	2	2	2	2	2	2	2	2	1.5
	WB-R	1	1	1	1	1	1	1	1	1	1
	SB-L	1	0.5	0.5	2	2	2	1	1.5	0.5	0.5
	SB-S	1.5	0.5	1.5	0.5	0.5	0.5	1	0.5	0.5	0.5
	SB-R	0.5	2	1	0.5	0.5	0.5	1	1	2	2

Note: Jun. denotes the junction ID, and Dir. denotes the direction of approach lane. When two directions traffic share one lane, the lane number of each direction is 0.5.

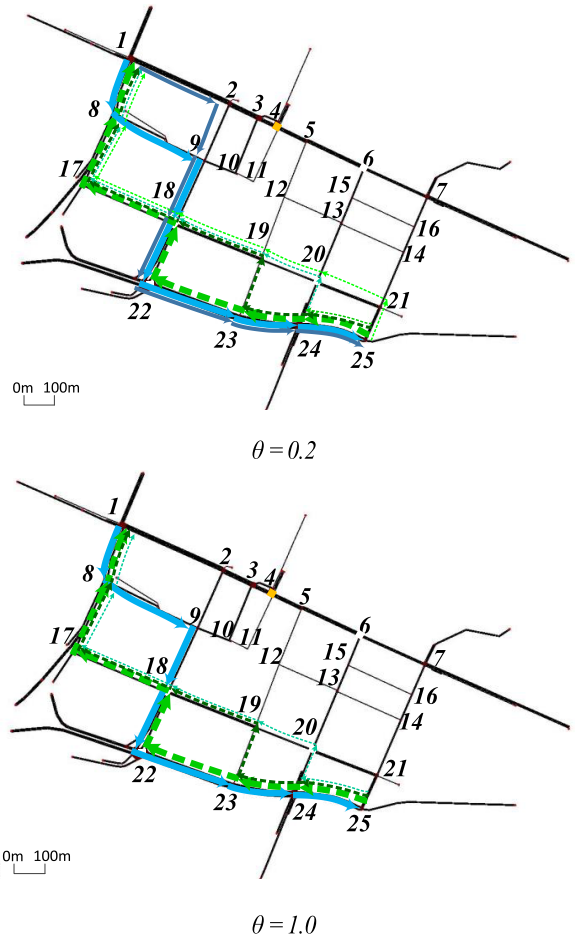

FIGURE 6. Route flow distribution when θ is 0.2 and 1.0.

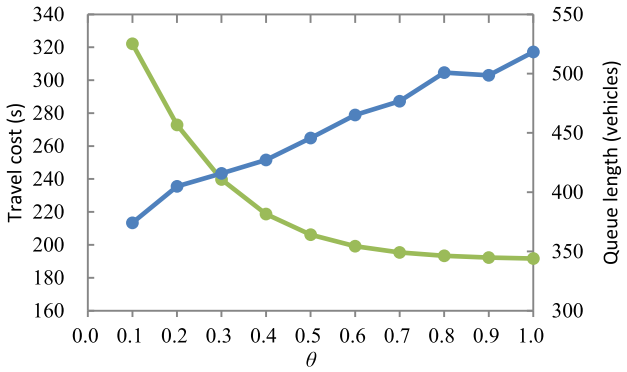

FIGURE 7. Average network impedance and queue length with different θ.

The average impedance (*i.e.* travel cost) and total queue length of the network in Experiment 2 are shown in Fig. 7. It can be seen that the average network impedance dramatically decreases at first and then stabilizes as θ is incremented. When $\theta \geq 0.6$, the average network impedance remains nearly identical. The average network impedance reduces by 130.45 s as θ increases from 0.1 to 1.0. However, the total queue length at signalized junction increases as θ is incremented because traffic will concentrate at some certain road sections to increase traffic flow at the approaches of signalized junctions. As a result, longer queues will appear at signalized junctions. The tendencies of average impedance and queue length in response to increment of θ indicate that travel time cost has a larger impact on traveler route choice than intra-junction time cost does.

V. CONCLUSIONS

To improve junction capacity and reduce time cost (impedance), this paper proposes an approach to dynamically

optimize reversible lane assignments for signalized junctions and a bi-level programming model. The lower model is a stochastic user equilibrium model used to compute the equilibrium traffic flow on a road network. According to the equilibrium traffic flow, the upper model gives the optimal reversible lane assignment, which is used as the input of the lower model for the next optimization iteration.

To validate the proposed model, this paper employs two numerical experiments. The first experiment uses a simple road network which has only 4 routes from origin to destination. The result shows that, despite using different traffic assignment models, the same optimal reversible lane assignment can be obtained. However, the stochastic user equilibrium model can determine the smallest average network impedance which is 7.8% smaller on average than other traffic assignment models. Moreover, the algorithm convergence speed is relevant to the impedance perception parameter θ. The algorithm convergence is faster with θ increment. When $\theta \geq 0.5$, the average network impedance is stabilized. Due to the small scale of the first experimental network, the convergence precision has little impact on the final optimal result.

The second experimental network is a field road network. According to the result, the optimized reversible lane assignment depends on the parameter θ. The larger the value of θ, the smaller the average network impedance. The average impedance decreases by 40% when θ increases from 0.1 to 1.0. The optimized reversible lane assignment when $\theta = 1.0$ is logically reasonable, so the validity of the proposed model can be proved.

In conclusion, by using the proposed approach to optimize the reversible lane assignment for junctions, the junction capacity can be improved and traveler time cost can be reduced. Furthermore, the proposed approach is expected to improve the operation of the entire urban road network with relatively small investment. In the future road network where self-driving cars and traditional human-driving cars coexist, the optimization of reversible lane assignments deserves further study.

REFERENCES

[1] L.-L. Li, Z.-W. Qu, Y. H. Chen, and D. H. Wang, "Control strategy of variable lane," *J. Jilin Univ.*, vol. 39, no. 1, pp. 98–103, Mar. 2009.
[2] B. Wolshon and L. Lambert, *Convertible Roadways and Lanes: A Synthesis of Highway Practice*, vol. 340. Washington, DC, USA: Transportation Research Board National Resear, 2004.
[3] B. Wolshon and L. Lambert, "Reversible lane systems: Synthesis of practice," *J. Transp. Eng.*, vol. 132, no. 12, pp. 933–944, Dec. 2006.
[4] A. Golub, "Perceived costs and benefits of reversible lanes in Phoenix, Arizona," *J. Inst. Transp. Eng.*, vol. 82, no. 2, pp. 38–42, Feb. 2012.
[5] J. Hemphill and V. H. Surti, "A feasibility study of a reversible-lane facility for a Denver street corridor," *Transp. Res. Rec.*, no. 514, pp. 29–32, Jan. 1974.
[6] H. Waleczek, J. Geistefeldt, D. Cindric-Middendorf, and G. Riegelhuth, "Traffic flow at a freeway work zone with reversible median lane," *Transp. Res. Procedia*, vol. 15, pp. 257–266, Jun. 2016.
[7] J. E. Upchurch, "Reversible flow on a six lane urban arterial," *Traffic Eng.*, vol. 45, no. 12, pp. 11–14, Dec. 1975.
[8] A. Karoonsoontawong and D.-Y. Lin, "Time-varying lane-based capacity reversibility for traffic management," *Comput.-Aided Civil Infrastruct. Eng.*, vol. 26, no. 8, pp. 632–646, Nov. 2011.
[9] B. Wolshon, "'One-way-out': Contraflow freeway operation for hurricane evacuation," *Nat. Hazards Rev.*, vol. 2, no. 3, pp. 105–112, Aug. 2001.
[10] B. Wolshon, "Planning for the evacuation of New Orleans," *J. Inst. Transp. Eng. (ITE)*, vol. 72, no. 2, pp. 44–49, Feb. 2002.
[11] E. Urbina and B. Wolshon, "National review of hurricane evacuation plans and policies: A comparison and contrast of state practices," *Transp. Res. A*, vol. 37, no. 3, pp. 257–275, Mar. 2003.
[12] J. Wojtowicz and W. A. Wallace, "Traffic management for planned special events using traffic microsimulation modeling and tabletop exercises," *J. Transp. Saf. Secur.*, vol. 2, no. 2, pp. 102–121, Jun. 2010.
[13] Y. Cao, Z. Zou, and H. Xu, "Analysis of traffic conflict characteristic at temporary reversible lane," *Period. Polytech. Transp. Eng.*, vol. 42, no. 1, pp. 73–76, Mar. 2014.
[14] G. Ren, J. Hua, Y. Cheng, Y. Zhang, and B. Ran, "Bus contraflow lane: Improved contraflow approach in freeway evacuation," *Transp. Res. Rec.*, no. 2312, pp. 150–158, Jan. 2012.
[15] G. Theodoulou and B. Wolshon, "Alternative methods to increase the effectiveness of freeway contraflow evacuation," *Transp. Res. Rec.*, no. 1865, pp. 48–56, Jan. 2004.
[16] G. Kalafatas and S. Peeta, "Planning for evacuation: Insights from an efficient network design model," *J. Infrastruct. Syst.*, vol. 15, no. 1, pp. 21–30, Mar. 2009.
[17] H. Tuydes and A. Ziliaskopoulos, "Network re-design to optimize evacuation contraflow," in *Proc. 83rd Annu. Meet. Transp. Res. Board*, Washington, DC, USA: NBS, Jan. 2004.
[18] H. Tuydes and A. Ziliaskopoulos, "Tabu-based heuristic approach for optimization of network evacuation contraflow," *Transp. Res. Rec.*, no. 1964, pp. 157–168, Jan. 2006.
[19] C. Xie and M. A. Turnquist, "Lane-based evacuation network optimization: An integrated Lagrangian relaxation and tabu search approach," *Transp. Res. C, Emerg. Technol.*, vol. 19, no. 1, pp. 40–63, Feb. 2011.
[20] C. Xie, D.-Y. Lin, and S. T. Waller, "A dynamic evacuation network optimization problem with lane reversal and crossing elimination strategies," *Transp. Res. E, Logistics Transp. Rev.*, vol. 46, no. 3, pp. 295–316, May 2010.
[21] H.-F. Xu, S.-S. Gao, Q.-M. Zheng, and K. Zhang, "Hybrid dynamic lane operation at signalized intersection," *J. Jilin Univ.*, vol. 48, no. 2, pp. 430–439, Mar. 2018.
[22] H.-Z. Zhang and Z.-Y. Gao, "Optimization approach for traffic road network design problem," *China J. Manage. Sci.*, vol. 15, no. 2, pp. 86–91, Apr. 2007.
[23] J.-B. Sheu and S. G. Ritchie, "Stochastic modeling and real-time prediction of vehicular lane-changing behavior," *Transp. Res. B, Methodological*, vol. 35, no. 7, pp. 695–716, Aug. 2001.
[24] J. Zhao, Y. Liu, and X. Yang, "Operation of signalized diamond interchanges with frontage roads using dynamic reversible lane control," *Transp. Res. C, Emerg. Technol.*, vol. 51, pp. 196–209, Feb. 2015.
[25] C. Krause, N. Kronpraset, J. Bared, and W. Zhang, "Operational advantages of dynamic reversible left-lane control of existing signalized diamond interchanges," *J. Transp. Eng.*, vol. 141, no. 5, p. 04014091, Dec. 2014.
[26] K. J. Assia and N. T. Ratroutb, "Proposed quick method for applying dynamic lane assignment at signalized intersections," *IATSS Res.*, vol. 42, no. 1, pp. 1–7, Apr. 2018.
[27] C. K. Wong and S. C. Wong, "Lane-based optimization of signal timings for isolated junctions," *Transp. Res. B, Methodological*, vol. 37, no. 1, pp. 63–84, Jan. 2003.
[28] J. Zhao, M. Yun, H. M. Zhang, and X. Yang, "Driving simulator evaluation of drivers' response to intersections with dynamic use of exit-lanes for left-turn," *Accid Anal. Prev.*, vol. 81, pp. 107–119, Aug. 2015.
[29] Z. He, L. Zheng, and W. Guan, "A simple nonparametric car-following model driven by field data," *Transp. Res. B, Methodological*, vol. 80, pp. 185–201, Oct. 2015.
[30] D. Ma, X. Luo, W. Li, S. Jin, W. Guo, and D. Wang, "Traffic demand estimation for lane groups at signal-controlled intersections using travel times from video-imaging detectors," *IET Intel. Transport Syst.*, vol. 11, no. 4, pp. 222–229, May 2017.
[31] Y. Sheffi, *Urban Transportation Networks: Equilibrium Analysis With Mathematical Programming Methods*. Englewood Cliffs, NJ, USA: Prentice-Hall, 1985, pp. 261–302.
[32] D. Ma *et al.*"Gating control for a single bottleneck link based on traffic load equilibrium," *Int. J. Civil Eng.*, vol. 14, no. 5, pp. 281–293, Jul. 2016.
[33] S. Wu and Z. Yang, "Optimizing location of manufacturing industries in the context of economic globalization: A bi-level model based approach," *Phys. A, Stat. Mech. Appl.*, vol. 501, pp. 327–337, Jul. 2018.

[34] M. Florian and C. Yang, "A coordinate descent method for the bi-level O-D matrix adjustment problem," *Int. Trans. Oper. Res.*, vol. 2, no. 2, pp. 165–179, Apr. 1995.
[35] L. Bianco, M. Caramia, and S. Giordani, "A bilevel flow model for hazmat transportation network design," *Transp. Res. C, Emerg. Technol.*, vol. 17, no. 2, pp. 175–196, Apr. 2009.
[36] E. Angulo, E. Castillo, R. García-Ródenas, and J. Sánchez-Vizcaínoc, "A continuous bi-level model for the expansion of highway networks," *Comput. Oper. Res.*, vol. 41, pp. 262–276, Jan. 2014.
[37] H. Shao, W. H. K. Lam, A. Sumalee, A. Chen, and M. L. Hazelton, "Estimation of mean and covariance of peak hour origin–destination demands from day-to-day traffic counts," *Transp. Res. B, Methodological*, vol. 68, pp. 52–75, Oct. 2014.
[38] J. Rong, M. He, and C. M. Chen, "Dynamic model of calculating queue length at signalized intersection," *China J. Highway Transp.*, vol. 15, no. 3, pp. 101–104, Jul. 2002.
[39] R. Akçelik, "Time-dependent expressions for delay, stop rate and queue length at traffic signals," Austral. Road Res. Board, Vermont South, VIC, Australia, ARRB Internal Rep. AIR 367-1, Sep. 2011.
[40] *Highway Capacity Manual*, Transp. Res. Board Bus. Office, Washington, DC, USA, 2010.
[41] F. V. Webster, "Traffic signal settings," Dept. Sci. Ind., Res. Road Res. Lab., London, U.K., Tech. Paper 39, 1958.
[42] D. Ma, X. Luo, S. Jin, D. Wang, W. Guo, and F. Wang, "Lane-based saturation degree estimation for signalized intersections using travel time data," *IEEE Intell. Transp. Syst. Mag.*, vol. 9, no. 3, pp. 136–148, Jul. 2017.
[43] D. P. Bertsekas, "Optimization algorithms: An overview," in *Convex Optimization Algorithms*, Nashua, NH, USA: Athena Scientific, 2015, pp. 55–58.
[44] C. Ma, R. He, and W. Zhang, "Path optimization of taxi carpooling," *PLoS ONE*, vol. 13, no. 8, pp. 1–15, Aug. 2018.
[45] P.-A. Chen and D. Kempe, "Altruism, selfishness, and spite in traffic routing," in *Proc. 9th ACM Conf. Electron. Commerce*, Chicago, IL, USA, 2008, pp. 140–149.
[46] J. G. Wardrop, "Some theoretical aspects of road traffic research," in *Proc. Inst. Civil Eng.*, vol. 1, no. 3, pp. 325–362, May 1952.
[47] Z. He, W. Guan, and S. Ma, "A traffic-condition-based route guidance strategy for a single destination road network," *Transp. Res. C, Emerg. Technol.*, vol. 32, pp. 89–102, Jul. 2013.

TING LU received the B.E. degree in traffic engineering from the Nanjing University of Science and Technology, Nanjing, China, in 2008, the M.E. degree in traffic information engineering and control from Jilin University, Changchun, China, in 2011, and the Ph.D. degree in transportation systems from the Braunschweig University of Technology, Braunschweig, Germany, in 2015. Since 2015, she has been a Lecturer with the Faculty of Maritime and Transportation, Ningbo University. Her research interests include traffic planning and control, intelligent transportation systems, urban logistics, and transport economics.

ZHONGZHEN YANG received the B.E. degree in aero survey and remote sensing engineering from Southwest Jiaotong University in 1986, the M.E. degree in aero survey and remote sensing engineering from the Dalian University of Technology in 1989, and the Ph.D. degree in transport engineering from Nagoya University, Japan, in 1997.

From 1997 to 2001, he was a Chief Researcher with the Nagoya Industrial Science and Technology Institute. From 2001 to 2017, he was a Professor with the Transport Management Department, Dalian Maritime University. Since 2018, he has been a Professor with the Faculty of Maritime and Transportation, Ningbo University. He has authored two books and more than 100 articles. His research interests include transportation planning, traffic control, urban logistics, and transport and shipping economics.

DONGFANG MA received the M.E. and Ph.D. degrees in traffic information engineering and control from Jilin University, Changchun, China, in 2009 and 2012, respectively. From 2012 to 2014, he was a Post-Doctoral Researcher with the Department of Civil Engineering and Architecture, Zhejiang University. Since 2015, he has been with the Institute of Marine Information Science and Technology, Zhejiang University. His current research interests include intelligent transportation systems, traffic planning and management, and big data mining.

SHENG JIN received the M.E. and Ph.D. degrees in transportation engineering from Jilin University, Changchun, China, in 2010. He is currently an Associate Professor with the College of Civil Engineering and Architecture, Zhejiang University, Hangzhou, China. He has published more than 50 articles in related journals, such as *Transportation Research Part A*, *Accident Analysis & Prevention*, the IEEE ITSM, and the IEEE T ITS. His research interests are focused on traffic flow theory, intelligent transportation systems, traffic signal control, and traffic big data mining.